Segregation of granular mixtures in a spherical tumbler

Tilo Finger,[1] Florian von Rüling,[1] Sára Lévay,[2] Bence Szabó,[3] Tamás Börzsönyi,[3] and Ralf Stannarius[1]
[1]*Otto-von-Guericke Universität Magdeburg, Institute for Experimental Physics, D-39016 Magdeburg, Germany*
[2]*Institute of Physics, Budapest University of Technology and Economics, H-1111 Budapest, Hungary*
[3]*Institute for Solid State Physics and Optics, Wigner Research Center for Physics, Hungarian Academy of Sciences, P. O. Box 49, H-1525 Budapest, Hungary*

(Received 25 October 2015; revised manuscript received 14 January 2016; published 8 March 2016)

Segregation of polydisperse granular materials in rotating containers is a ubiquitous but still not satisfactorily understood phenomenon. This study describes axial segregation of bidisperse granular mixtures of glass beads in a spherical container, rotating about its horizontal axis. Depending on the filling fraction of the mixer and on the composition of the mixture, qualitatively different spontaneously formed patterns are observed. For technical applications, the well-localized segregated bands allow a convenient separation of individual components of the mixtures. It is particularly surprising that the initial compositions of the granular mixtures have a fundamental influence on the location of the segregated bands. This evidences a collective pattern forming mechanism. The spontaneous formation of these bands cannot simply be traced back to individual particle dynamics. Existing models for segregation in spherical mixers are critically examined and extensions are suggested.

DOI: 10.1103/PhysRevE.93.032903

I. INTRODUCTION

It is well known that agitated granular mixtures tend to spontaneous segregation in many situations. This may often be an undesired side effect in mixers, but it also holds the potential for applications, when demixing and an extraction of individual compounds is intended. The horizontally rotating cylindrical drum partially filled with grains of different sizes and/or densities has become one of the standard systems for the study of spontaneous pattern formation in granular matter. The phenomenon of spontaneous axial segregation in cylindrical tumblers has been known for decades. Oyama [1] described this effect in a pioneering study in 1939. Rotating mixers of various geometries and different types of granular materials were investigated since then [1–57]. But irrespective of this long (and yet incomplete) list of published experimental and theoretical studies, even fundamental features of the grain dynamics have been incompletely understood until now.

In long cylindrical or rectangular mixers, three types of segregation have been described. After a few rotations, the material demixes radially [2,3] by size. This is a well understood process. The smaller particles form an axial core. Then, an instability of this core can lead to axial band patterns [1,4–6]. These appear typically after a few dozen rotations of the mixer, but only for certain combinations of grain and tumbler sizes and geometries. Recently, particle interactions were suggested as possible origin of this axial banding [7]. The band pattern coarsens in the course of several thousand rotations [8–10] by the merging of neighboring bands.

Some experiments, particularly studies of radial segregation [2,3], have been performed in very short, quasi-2D drums, and a much larger number of studies have dealt with very long cylinders where the influence of the lateral caps can be neglected. However, effects of the lateral ends have been noticed and described (see, for example, Refs. [10–15]). It has been suggested that axial segregation is triggered by end-wall effects. The influences of the flat end walls of the tumbler on pattern onset have been clearly demonstrated and studied quantitatively. Numerical simulations by Arntz *et al.* [13] suggest that particles with lower friction form bands near the tube ends. Influences of the lateral container walls in short cylinders were computed numerically by Chen *et al.* [14,15]. Particularly, the effects on velocity fields and particle trajectories were described in that study.

Technical applications, e.g., in a pharmaceutical industry [58], often involve short, compact mixers where the end walls play a crucial role in segregation. These influences are particularly evident when instead of a cylindrical geometry, spherical mixers are used [16–21]. In spherical tumblers with high fill level, bidisperse mixtures were found to segregate such that large particles accumulate at the lateral poles (intersections of the rotation axis with the container wall). When the fill level is gradually lowered, one finds an interesting transition of this large-small-large (LSL) three-stripe pattern to an inverse, small-large-small (SLS) configuration. In the latter, the large beads form a central band while the smaller beads occupy the poles. Additionally, they always form a core channel traversing the mixer. This behavior has been discovered and described in two earlier publications [17,18]. Chen *et al.* [18] studied 50%:50% bidisperse mixtures of $(1+2)$, $(1+3)$, $(1+4)$, and $(2+4)$ mm sized glass beads, respectively, in a sphere of 14 cm diameter. They found transitions from LSL to SLS with decreasing fill levels of the mixer in all four combinations, and for all rotation rates between 2 rpm and 20 rpm, by optical observation of the granular bed surface. The critical fill level for the pattern inversion depends on the size ratio of container and particles, and as a rule it occurs at higher fill levels for larger grain sizes. For the smallest grains, it is found between 20% and 30% fill level, while for the largest grain size it occurs between 50% and 60% fill level. The degree of segregation improved with rotation rate. The authors performed a numerical simulation, and its results were in qualitative agreement with the observed experimental patterns. Individual particle trajectories were extracted from the simulations.

At the same time, Naji *et al.* [17] reported similar observations in a tumbler of 37 mm diameter: The beads were 0.55 and 1.5 mm, respectively, in a 50%:50% mixture. In these experiments, the granulate was fully immersed in

water. It is well established that an immersion liquid does not change the segregation scenarios qualitatively but only quantitatively [10,24]. Optical investigations of the granular bed surface in the sphere were accompanied by magnetic resonance imaging of the complete granular bed. The observed segregation structures and transitions were qualitatively the same as those reported in Ref. [18]. In addition, it was shown that the change of container size to bead size influences the threshold for the LSL-to-SLS transition. In larger containers, the transition is found at lower fill levels. This is in full agreement with the trends reported for different grain sizes at constant container diameter [18].

Both of these studies dealt only with 50%:50% mixtures (by volume) of the two grain types. In particular, all numerical simulations were performed for an equal volume share of the two components, which is in practical situations a rather exceptional case. A priori, it would seem quite natural to assume that the trend to form LSL or SLS patterns should not sensitively depend on this composition. However, when reducing the share of large grains in the mixture for particle tracking purposes, we discovered an unexpected phenomenon that is quantitatively investigated in this study: The mixture composition plays a crucial role in the pattern selection process. This observation appears to be counterintuitive: Existing models that describe spontaneous segregation in rotating mixers often consider the trajectories (diffusion or drift) of individual particles. For example, Chen *et al.* [18] explained the SLS patterns observed in their experiments and simulations by differences in the trajectories of individual small and large spheres. They based their explanation on the obtuse angle between the container wall and the flowing layer at low fill levels, which leads to the formation of a monolayer of beads at the container wall, above the flowing plane. The monolayer is mainly built of small beads, which fall into the flowing layer and, according to that model, force the larger ones towards the equator. On the other hand, a drift of the large particles towards the poles was found during the formation of LSL patterns at high fill levels. Naji *et al.* [17] independently proposed a different model of SLS pattern formation, which also started from assumptions on individual particle trajectories.

In cylindrical mixers, size segregation into banded patterns has been attributed to the differences of dynamic angles of repose for different compositions of the mixture in different parts of the tumbler [5,6,27,28]. Recently, another source for size segregation in flowing layers was identified by Fan and Hill [59,60]. We will discuss its relevance for the rotating sphere below.

The present study shows that in the spherical tumbler, different pattern selection processes are effective for individual large beads or small numbers of large beads on the one hand and for sufficiently large amounts of them in the mixture on the other hand. The type of segregation pattern that is formed depends sensitively upon the composition of the mixture. In cylindrical mixers, a study of the influences of the composition of bidisperse mixtures on segregation processes was reported by Juarez *et al.* [22]. They found that for very small concentrations of large particles, isolated single bands formed. The long-term coarsening dynamics was found to differ from the logarithmic signature in 1:1 mixtures. However, the above-mentioned phenomena in spherical mixers go much beyond this observations in cylindrical tubes. In the spheres, not only the width and long-term dynamics are affected, but also the spatial arrangement of the bands is determined predictably by the sample composition.

II. EXPERIMENT

The mixers used in this study are spherical transparent plastic containers with diameters of 37 mm, 66 mm, and 73 mm. A lateral fitting is attached to the outside of each sphere, connecting it to a stepper motor. The rotation axis is horizontal. Figure 1 sketches the experimental setup, together with a typical image of the filled container. The granulate shown in the image is a bidisperse 50:50% (by volume) mixture of transparent glass spheres with diameters in the range from 0.5 mm to 0.63 mm (S) and amber (orange) larger spheres (L) with diameters in the range from 1.4 mm to 1.6 mm. In the

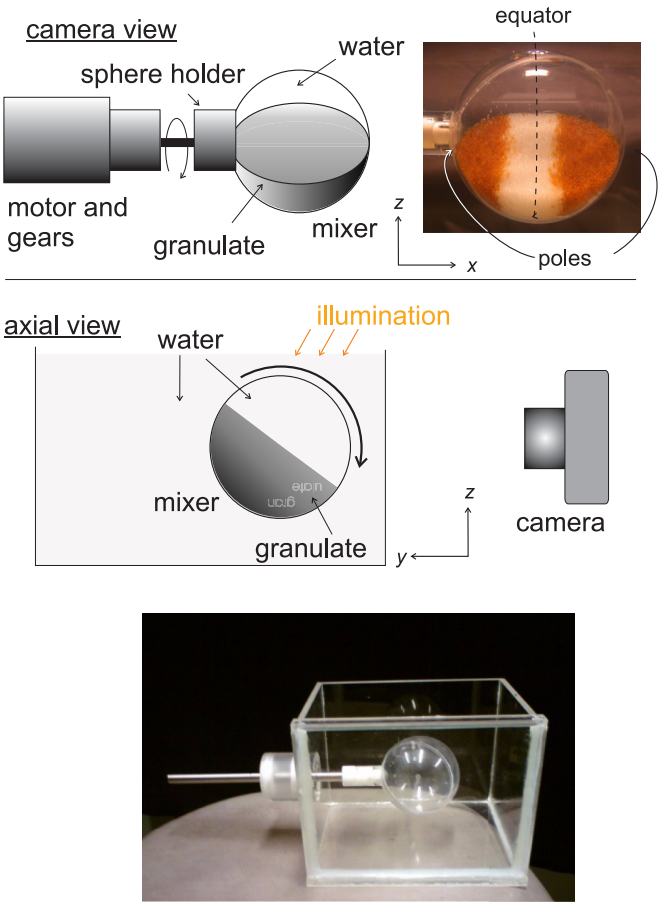

FIG. 1. Sketches of the experimental setup, consisting of the mixer, a gear motor, light source and camera. In most experiments, the sphere rotates such that upper part moves towards the camera. Then, the flowing plane is imaged. In some experiments, the rotation sense is reverse. For the distinction of the structures, this detail is irrelevant. The upper right image shows a 73 mm diameter sphere after segregation at 10 rpm. The white equatorial band consists of small beads, the darker polar regions of large beads (LSL pattern), their percentages in the mixture were 50%:50%. The bottom picture shows the empty setup without the motor.

following, we study mixtures of these L and S spheres mixed in different ratios $\gamma : (1 - \gamma)$. The densities of the grains are practically equal.

The rotation speed of the sphere is varied between 2 rotations per minute (rpm) and 30 rpm. This restricts experiments to a dynamic range of rotation rates where the granulate flows continuously. The rate is slow enough to avoid ballistic particle motion and fast enough to be beyond the avalanche regime. In the observed rotation rate range, there is no measurable slip between the container and the beads in the outer layer. The ratio of centrifugal forces on the grains and gravitational forces was in all experiments below 0.05, typically of the order of 10^{-3}.

Images of the flowing plane of the granular bed are recorded with a digital camera, either a Nikon Coolpix 4500 digital camera, controlled by a computer (using KRINNICAM software) or an Canon EOS 600D. The images are stored at regular intervals (usually 1 min) or after the rotation has been stopped. In some experiments, video sequences with a frame rate of 60 fps were recorded with the EOS camera. The typical spatial resolution is 10 pixel/mm or better in all images. Typical experiments run for about 100 revolutions of the sphere, and in a few cases we have recorded the long-term behavior, up to 10 000 rotations.

After filling the container with the granulate, it is completely filled up with water. The purpose is to avoid static electricity and to achieve comparable conditions to previous measurements [17]. Often the rotation of the mixer releases small bubbles of air that collect inside at the top of the sphere. We did not take care to remove these bubbles since they are sufficiently far from the granular bed and have no influence on the observations. In some of the images they appear in the viewing field. In order to compensate optical distortions from refraction at the sphere borders, the spherical mixer is completely immersed in a cuboid water-filled tank, with transparent sides (Fig. 1, bottom).

The filling levels ϕ of the mixers given in the text refer to the volume of the components in demixed state (including all voids between the beads) divided by the container volume. After initial mixing, this fill level is slightly lower because packing in the mixed state is more efficient.

III. RESULTS

A. Influence of the mixture composition

Previous experiments by Naji [17] were performed at a fixed composition $\gamma = 50\%$. In the present investigation, we were interested primarily in the influence of different compositions. Figure 2 shows the fundamental finding of our study in a rough overview of the observed patterns. The images were recorded at 3 rpm rotation speed of the mixer. Dark (amber) regions correspond to the bands of large beads. The vertical arrow sketches the mixture composition and variation of fill levels in previous experimental studies [17,18] (different mixer, different rotation rates, different materials).

The important new observation is that the change of the composition has similarly strong consequences as the change of the container fill height, selecting qualitatively different segregation patterns. We observe LSL (or SLSLS, see below) patterns independent of fill heights at sufficiently low concentrations of the large spheres. This is evident in particular when only few large beads were present: These gather near (but not always exactly at) the poles.

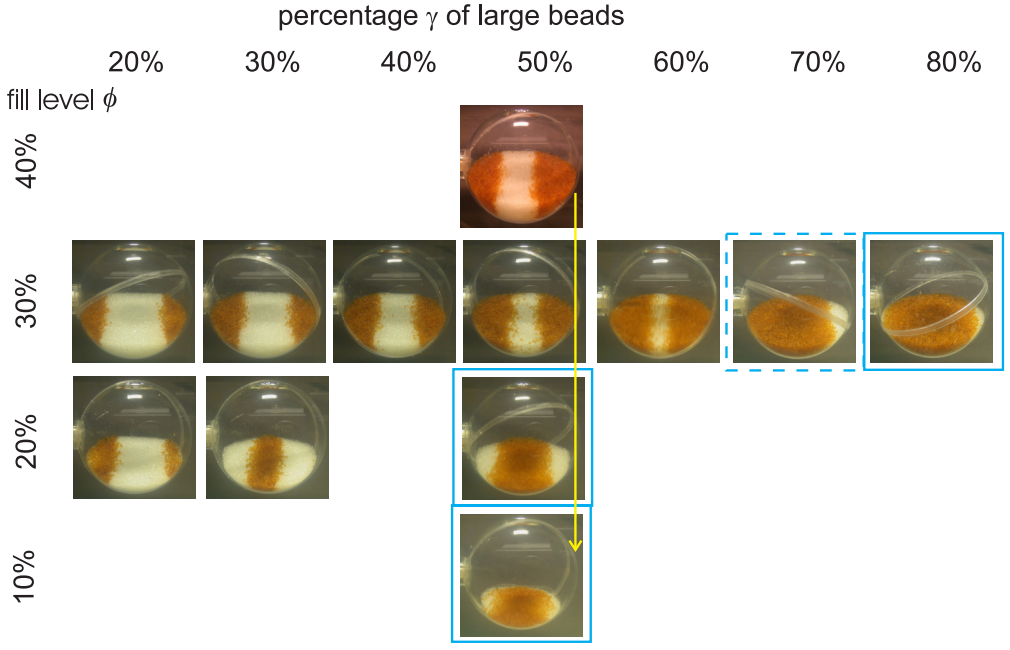

FIG. 2. Segregation patterns in a 73 mm diameter spherical mixer for different fill levels ϕ and mixture compositions γ (views of the flowing plane). Blue solid frames label SLS patterns, the dashed frame marks an image in the transition range. In all experiments, the small beads form an axial core structure that penetrates the whole sphere. The images were recorded after typically 100 revolutions of the sphere, starting from a mixed state. After this period, no further pattern dynamics was observed for at least 1000 revolutions. Some long-term dynamics will be described below. The rotation speed is 3 rpm, flow is from top to bottom in the images

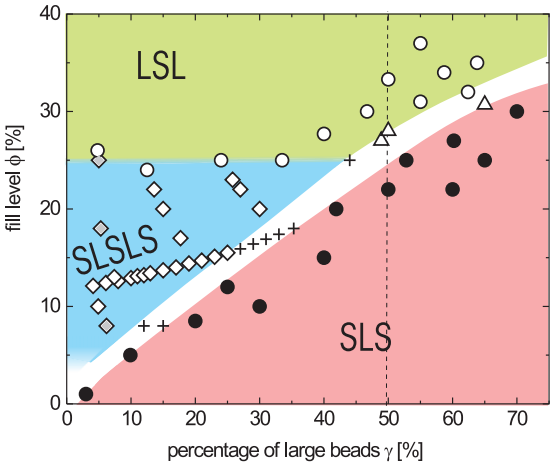

FIG. 3. Influence of the fill level ϕ and sample composition γ in the 73-mm mixer at 6 rpm rotation speed. Open circles denote LSL, filled circles denote SLS patterns, and diamonds denote measurements in the SLSLS region. Crosses represent measurements in a transition range from SLS to SLSLS. The triangles denote patterns in the SLS/LSL coexistence range. The shaded areas roughly sketch the extensions of the regions where the three pattern types are found. The three diamonds with light gray shades correspond to the images shown in Fig. 4(a).

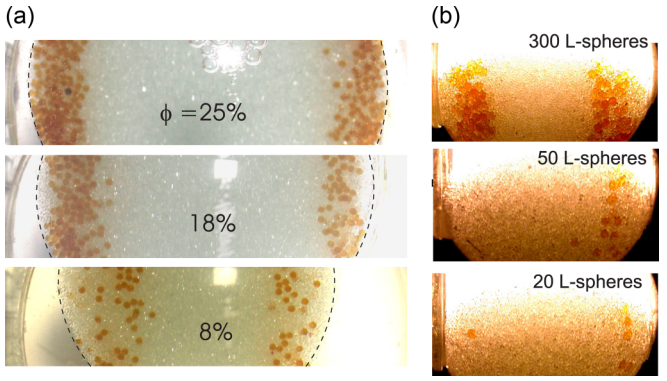

FIG. 4. SLSLS five stripe patterns. Two separated L bands form in the sphere, the equator and poles are occupied by small grains, and the L spheres assemble in two bands, which are clearly separated from each other. (a) A 73-mm container at 6 rpm, $\gamma \approx 5\%$. With increasing container fill level ϕ, the bands move outward and finally reach the LSL configuration. At $\phi = 25\%$, the LSL type pattern is practically reached. (b) A 37-mm container at 10 rpm, $\phi = 30\%$ the numbers of L beads in the mixture (given in the images) correspond to $\gamma = 12.6\%$ (300 L beads), 2.1% (50 L beads), and 0.84% (20 L beads), respectively. Even when γ approaches zero, trajectories of single large spheres remain confined in the same two regions.

Figure 3 gives a quantitative overview of the structures observed in the 73 mm spherical mixer for different fill levels and sample compositions. They were recorded at a rotation rate of 6 rpm, and thus the regions where the individual pattern types are found slightly differ from those in Fig. 2 (see Sec. III C). Three fundamental pattern types can be distinguished. At low fill levels and large percentages of L beads, γ (red shaded area in the figure), SLS band patterns are found. At high fill levels, one finds LSL patterns for all investigated concentrations γ. This area is shaded green in the figure. In the third region one finds two mirror-symmetric bands of L beads embedded between an equatorial and two polar regions of S beads. This region (SLSLS) is shown as blue in the figure. In Fig. 4, typical segregation patterns in that region are shown as a function of ϕ [Fig. 4(a)] and γ [Fig. 4(b)]. The position of the bands shifts towards the poles when ϕ increases [Fig. 4(a)]. On the other hand, their positions remain essentially unchanged when the fill level ϕ is kept constant but the composition γ of the granular mixture is varied within the SLSLS parameter range. The two symmetric bands are not necessarily equally populated. The L grains appear to be statistically distributed between both bands, so at low γ, one may have large differences between the numbers of particles in each band [see Fig. 4(b)]. We note that in the SLSLS pattern, the poles are occupied solely by small particles. This excludes the hypothesis [17] that the reduction of friction at the poles drives the migration of the larger spheres out of the equatorial region, at least in the SLSLS parameter range.

Between these three fundamental regions (SLS, LSL, and SLSLS), there exist certain transition ranges, which are left white in the graph of Fig. 3. It is evident in that plot that the transition from SLSLS to LSL is rather independent of γ. A threshold is not easy to determine exactly, because with increasing fill level ϕ, the two L bands shift outwards and the transition from SLSLS to LSL is practically continuous ("second order"). This transition is seen in Fig. 4(a).

Between the SLS and SLSLS regions (small ϕ,γ), there is a narrow parameter range with nonstationary, or less well-defined, segregation patterns (crosses in Fig. 3). This has been described earlier [17] for the fill-level dependence. Within a range of about 10% between these regions, either a single L band is formed that is shifted out of the equatorial plane or the pattern switches between different configurations. In situations where a single off-equatorial stripe is formed, both axial sides are equivalent, and one side is selected spontaneously. The stripe with large beads can even switch in such structures to the other side of the equator during few hundred rotations, i.e., the L particles may successively pass the S band at the equator to form a stripe at the mirrored position. This distinguishes the stripe dynamics in spherical mixer geometry qualitatively from that in a cylindrical drum, where bands of small beads are practically impenetrable to large spheres at this size ratio [9,36].

The change between LSL and SLS (large ϕ,γ) has the character of a direct "first order" transition, i.e., there is a narrow region where both patterns may coexist. The sample either develops three L bands or fluctuates between LSL and SLS patterns. This region is marked by triangles in Fig. 3.

B. Temporal evolution

The formation of the patterns occurs typically over a period of about 30 to 100 rotations. After that, the segregation bands are stable. For some segregation structures, one can also observe a long-term dynamics over several thousands of revolutions of the mixer (see below). We assume that, similarly to the cylindrical geometry, separate mechanisms are responsible for the initial segregation of the granulate into bands and for the long-term merging of individual segregated

bands (cf. Ref. [36]). For the selection of the pattern type, it does not matter whether the experiment starts with a well-mixed state or with any other initial pattern.

From a completely mixed state, the large grains first leave the axial core and emerge in the flowing layer. Initially, they are uniformly distributed on the flowing surface. At the same time, the small grains form an axial core that extends from one pole to the other. Thereafter, stripe formation sets in. For example, when ϕ and γ are within the SLS parameter range, the polar regions first become free of large grains. A broad equatorial L band forms, it narrows until it reaches a stationary width. Five snapshots of this process are shown in Fig. 5, right. The asymptotic width of this stripe depends on the mixture composition, and it is broader for larger γ. In the SLSLS parameter range, the process also starts with a certain accumulation of large grains in the equatorial region, as seen in Fig. 5, left. After a few rotations, the polar regions are completely free from L particles. Then, two lateral L stripes gradually form and the L grains accumulate there, while the equatorial region empties from L grains. The width of the two L bands also depends on the sample compositions; at larger γ the stripes are broader (Fig. 2). This behavior suggests that there are two competing processes, a fast one which leads to the accumulation of L grains in the central region and a slower one that redistributes these grains out of that region.

The pattern dynamics can be more complex in the transition ranges from SLS to SLSLS or to LSL. The band structure can fluctuate between different states, and individual bands can dissolve or reform, where individual configurations persist for dozens to several hundred rotations.

In addition to this initial evolution, one can also observe a long-term dynamics at much longer time scales, similar to the coarsening in cylindrical drums. In some long-term observations of initially two L stripes, one of the symmetrically arranged stripes of large beads dissolved and the complete L material was transported to the other one. These processes occur over periods of several thousand rotations. They are not considered here.

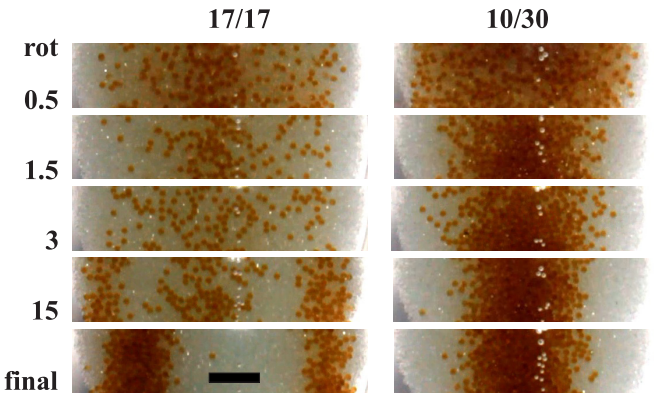

FIG. 5. Formation of the patterns: Snapshots after 0.5, 1.5, 3, and 15 rotations, and the final stationary pattern. The images show the central region with the full width of the flowing layer and a height of 1.25 cm. The scale bar is 1 cm. Left: SLSLS pattern at $\phi = 17\%, \gamma = 17\%$. First, the L grains leave the polar regions and assemble in the equatorial range, and then two lateral bands form and the central band empties. Finally, two symmetrically positioned L bands remain. Right: SLS pattern at $\phi = 10\%, \gamma = 30\%$; one central stripe forms by contraction of the area covered by large grains.

C. Effect of the rotation rate

The described structures exhibit rather little sensitivity to the rotation speed. The complete formation of the described segregation patterns is observed at rotation rates as low as 3 rpm. The quality of segregation slightly changes with rotation rates. The patterns are qualitatively the same at the fastest rotation rate studied here, 20 rpm, but the boundaries between the bands are less sharp and the segregation under fast spinning is not as perfect as at lower rates (Fig. 6). At very low rotation rates, in the avalanche regime, where the flow of particles on the slope is discontinuous, there is only a weak segregation effect. When the sphere is rotated at rates well above 20 rpm, the granulate mixes again and the segregation bands vanish.

The overall structure of the pattern state diagram in Fig. 3 is qualitatively representative for all rotation rates between 3 rpm and 18 rpm, but the transitions between the different segregation regimes slightly differ by a few percentages in both γ and θ (compare, e.g., Fig. 2, recorded at 3 rpm and Fig. 3, recorded at 6 rpm).

The weak influence of the rotation rate in a large parameter range is in agreement with the findings of a comprehensive investigation of fill level and rotation rate effects in cylindrical drums [25]. The destruction of the patterns at very high rates where the granulate enters the ballistic dynamic regime is also intuitively clear. When the particles perform ballistic trajectories, they leave the flowing layer. Then selection mechanisms in the flowing layer that drive segregation are no longer effective.

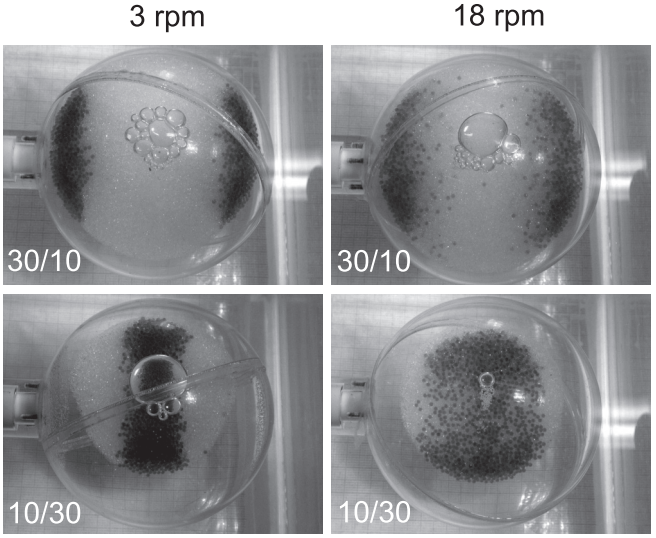

FIG. 6. Influence of the rotation speed on the quality of segregation: At low rotation rates, the patterns are better segregated, both LSL (top row: $\phi = 30\%$ fill level of the container, $\gamma = 10\%$ relative percentage of large spheres) and SLS (bottom row: $\phi = 10\%$, $\gamma = 30\%$). With increasing rotation rates, the segregation patterns become more "fuzzy." Sphere diameter 73 mm, rotation rates 3 rpm (left), and 18 rpm (right).

D. Container size effects

Experiments with different container sizes reveal the same qualitative structure of the pattern state diagrams but also some systematic trends in the existence ranges of the patterns. The transition ranges in the smaller (66 mm and 37 mm) mixers have not been determined systematically, but sampling the parameter space in the 66 mm sphere showed that all transitions changed to higher ϕ with decreasing container diameter (i.e., decreasing ratio of container size to bead size). For example, the 50 %:50 % mixture shows the transition from SLS to LSL between $\phi = 35\%$ and 40%. Comparison with published measurements of the 37 mm sphere in Ref. [17] shows that at further reduction of the sphere to particle size ratio, this trend continues. In Naji's experiments, the SLS-to-LSL transition took place between $\phi = 40\%$ and 50%. These shifts of the transitions to higher fill levels with a lower container-to-grain size ratio is in agreement with the observations in Ref. [18], where different grain sizes were studied in one and the same container.

E. Flow profile

In order to identify potential mechanisms that may lead to size segregation in the flowing layer [59,60], an analysis of the velocity profile of the surface flow was performed. Gradients of the in-plane flow velocity will naturally exist along the axial coordinate. This was demonstrated in an earlier analysis of the down-slope flow in a spherical mixer filled with dry granulate [21]. The authors reported an elliptical profile of the streamwise flow in the midpoint of the flowing layer as a function of the axial position.

The local flow profile in our system was determined quantitatively by means of particle image velocimetry. This has been performed in the 73-mm container at 6 rpm. A few red tracer particles were added to S grains. The result is shown in Fig. 7 on a grid of 3.2 mm $\times$3.2 mm for a 40% filled mixer with $\gamma = 0$. We present here only the velocity component

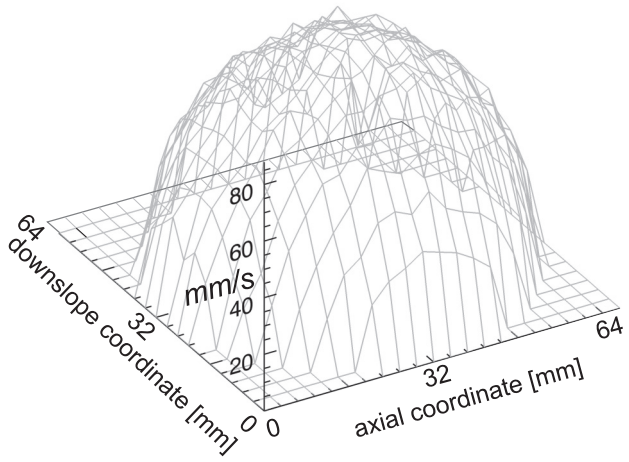

FIG. 7. Downslope component of the local flow velocity along the flowing layer plane in a 73-mm container filled with small grains, $\gamma = 0$, rotation speed 6 rpm. Flow profile (in mm/s) for $\phi = 40$ % fill level. The spatial coordinates extend cover the complete area of the fluidized layer, grid size 3.2 mm $\times$ 3.2 mm.

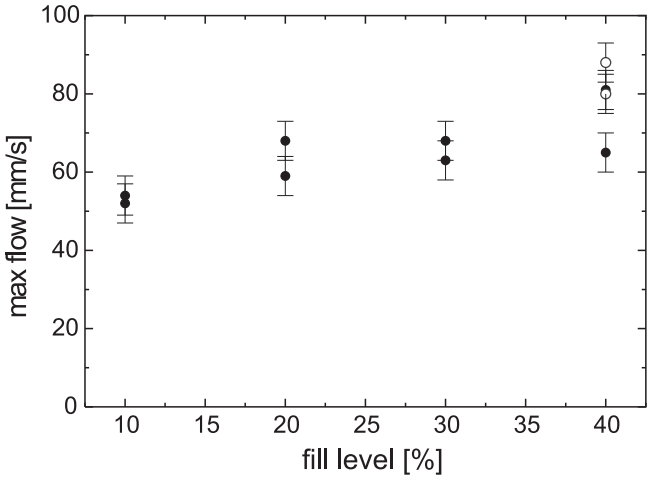

FIG. 8. Maximum flow velocity on the fluidized plane at different fill levels for samples with $\gamma = 0$ (filled symbols) and $\gamma = 2.5\%$ (open symbols) in a 73-mm sphere, rotating at 6 rpm.

down the slope, and the lateral velocity component in this experiment is approximately one order of magnitude smaller. Particles entering the flowing plane near the equator move faster than those closer to the poles, thus there are substantial shear gradients on both sides towards the poles. The velocity profile in the midplane is in perfect qualitative agreement with results reported by Pohlman [21] for dry monodisperse granulate in a spherical mixer.

There is only a weak dependence of the peak velocity on the filling fraction of the sphere in the investigated fill range of $10\% < \phi < 40\%$ (Fig. 8). The maximal flow velocity drops systematically from about 80 mm/s at $\phi = 40\%$ to about 55 mm/s at $\phi = 10\%$. The overall flow profile remains qualitatively unchanged.

These velocities have been determined for containers containing only small particles. A few L spheres, when added to a bed of S grains, move slightly faster, but the velocity differences are not significant. The two data points at $\phi = 40\%$ with $\gamma = 2.5\%$ represent an average velocity of the large and small spheres.

The most important conclusion from these measurements is that there exists a strong axial shear gradient in the flowing plane. Fan and Hill [59,60] concluded from numerical simulations and experiments that flow gradients can have important consequences for the segregation of size-dispersed granular mixtures. In dense systems as the ones studied here, the large particles have a stronger tendency to drift into regions with large shear gradients. The flow profile in Fig. 7 indicates that shear gradients in the flowing plane increase towards the polar regions. This peculiarity thus provides a mechanism to drive large grains out of the equatorial zone. Its relevance will be discussed below.

The individual particle trajectories of the colored large spheres are best visualized when multiple exposures of the container are superimposed. Qualitative observations are shown exemplarily in Fig. 9 for a low fill level and a low concentration of large beads. Figure 9(a) was recorded shortly (1.78 rotations) after the start of the experiment, when the initial mixed state still existed (between 1.78 and 1.82

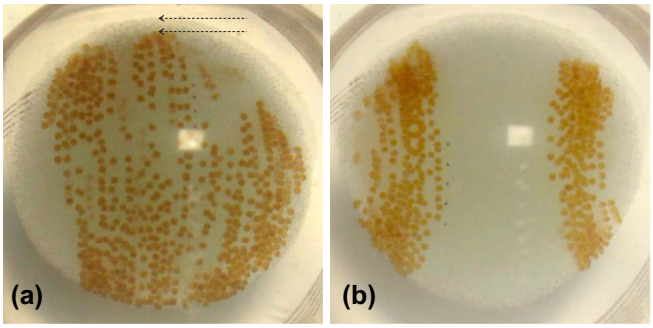

FIG. 9. Trajectories of particles visualized by overlay of successive video frames, $\phi = 8\%, \gamma = 6.2\%$, (a) in the initial mixed state after $\approx$1.8 rotations and (b) in the stationary SLSLS pattern after about 50 rotations. The rotation speed is 6 rpm, and the sphere diameter is 73 mm. At the upper edge of the flowing layer, a thin surface layer of small beads with an elevation of about 3 mm covers the rear container wall (dashed arrows).

sphere rotations), 25 frames recorded at a rate of 60 fps were superimposed. Figure 9(b) was taken after the stationary SLSLS pattern had formed. In both images, it is evident that the upper edge of the visible granular surface contains only small spheres. This is a thin boundary layer which is pushed up at the container wall above the flowing layer due to the obtuse angle between flowing plane and container wall [18]. It exists only at low fill levels. The dynamics of S grains that fall out of it was identified by Chen *et al.* [18] as one of the mechanisms favoring SLS patterns.

The essential difference between the two situations [Figs. 9(a) and 9(b)] is the shape of trajectories of the large grains. Initially, they flow in a similar way as indicated in Chen's paper. When the L stripes have formed, the bend of the trajectories is inverted. This inversion may be relevant for the stability of the SLSLS patterns.

IV. DISCUSSION

On the basis of the observations described in the previous section, one can draw the following conclusions: The segregation patterns in rotating spherical tumblers depend not only on the fill level, as noticed in earlier studies [17,18], but also crucially on the amount of large spheres in the mixture. Even a small change in the composition of the mixture (of a few percentages) may reverse the band pattern. Thus, one has to look for a collective effect: The trajectories of individual grains that form the segregation structures are not independent of the concentration of the components. The presence of multiple large grains, in particular in compact bands of L beads, influences the dynamics of the very L grains in the mixer, such that different regions of attraction may exist for individual particle trajectories, even when the container geometry, rotation dynamics, and fill level are identical.

In the light of the present experimental results, we revisit and re-evaluate the mechanisms proposed earlier for the selection of the patterns of 50%:50% bidisperse mixtures in the spherical tumbler and suggest further mechanisms that have to be considered. First, it seems that the profile of the velocity field in the flowing layer is an essential component for the observed segregation. The formation of patterns that contain small particles in the equatorial plane (LSL and SLSLS) can be explained if one considers recent numerical and experimental results by Fan and Hill [60]. They observed that at high solid fractions of the granulate, binary size-dispersed mixtures show a tendency to segregate such that the larger species accumulates in regions of high shear gradients of the flow. Considering the velocity profile shown in Fig. 7, it is evident that the flow profiles in spherical mixers contain substantial in-plane shear. The flow profile is much more influenced by the container geometry than in (long) cylinders (cf. also Ref. [21]). The absolute value of the shear gradient increases towards the lateral poles, while it is zero (for symmetry reasons) in the equatorial plane. This provides a strong tendency for the larger component (L spheres) to leave the equatorial plane towards the polar regions. This mechanism (abbreviated as SG for shear gradient) will be effective for single L spheres as well as for ensembles of large spheres as long as the velocity profile remains qualitatively the same. We assume that this is the main process that destroys SLS patterns. This shear-gradient mediated drift is present at all fill levels. Our measurements with monodisperse fillings show that there is little influence of the fill height of the container on the flow profile. The addition of small amounts of large spheres has little effect on the velocity profile.

A competing mechanism (BS for back sheet) that stabilizes structures with small grains in the polar regions (SLS and SLSLS) has been identified by Chen *et al.* [18]. At low fill levels, the thin layer, or even monolayer, of particles carried up above the flowing layer at the rear container wall contains only small grains (see Fig. 9). It was found that these grains fall out of the background layer preferentially towards the polar regions. Thus, containers with low fill levels prefer SLS patterns.

It was assumed earlier [17] that LSL patterns are caused by the reduction of friction at the end walls of the spherical container (similar to observations in cylindrical mixers [13]). When a container has a sufficiently high fill level, the large grains will have a preference to accumulate near the almost vertical container ends in the sphere mixer. This may explain that a large fill ratio ϕ supports the stability of LSL patterns. This mechanism (SV for sieving) is closely related to the shear driven migration effect, since the shear gradient in the flowing plane is largest near the lateral ends of a cylinder mixer or near the polar regions of a spherical mixer. However, the effect cannot explain the observed axial drift (not random diffusive motion) of isolated large spheres out of the equatorial region in a bed of small particles. Thus the end wall effect can only be an assisting stability factor, not the primary driving mechanism. Moreover, there is a continuous transition between LSL and SLSLS patterns with fill level changes. The driving mechanism for SLSLS patterns cannot be related to the reduction of friction at the polar walls since those regions are free of large grains at sufficiently low L grain concentrations for all fill levels. Thus, the explanation given in Ref. [17] is at least incomplete.

The conclusion drawn from these considerations is that at high fill levels, the drift of large grains into zones of high shear gradient is essential for the formation of structures with equatorial bands of small spheres (LSL and SLSLS). Sieving of small grains into deeper zones (Brazil nut effect) may also

support these patterns, particularly at high fill levels where the depth of the granular layer is large [17].

The formation of structures with L grains in the equatorial zone (SLS) has been explained by the existence of a thin sheet of grains transported with the back wall of the container above the flowing layer [18]. This sheet contains nearly exclusively small spheres (Fig. 9). This BS mechanism works best when the rear container wall forms a small angle with the horizontal, i.e., at low fill levels of the mixer. The sheet does not exist at high fill levels (around 40% and above), and indeed, at high-enough fill levels, SLS patterns are absent.

Interestingly, the stripe arrangement in the SLS pattern with respect to the local mixer radius is opposite to that observed by Zik *et al.* [28] in a nearly cylindrical long mixer with modulated radius. There, the large grains were found preferentially in the necks and the small particles in the bellies of the mixer. These experiments were performed at 50% fill level, where the BS mechanism is negligible. Probably there is also an axially modulated flow field in the axially modulated cylinder, but a simple explanation of segregation based on the SG mechanism fails there for symmetry reasons.

An unsolved question is the existence of SLSLS band patterns. Probably two competing effects contribute to their formation. The SG effect drives large grains out of the equatorial plane, and the BS mechanism supports the accumulation of small beads in the polar regions. The SLSLS pattern may form as a compromise between these two. When the fill level of the mixer increases, the BS mechanism ceases and the shear gradient related drift of the large grains dominates, leading to LSL structures. There is almost no dependence of the SLSLS-to-LSL transition on the mixture composition, which is in agreement with that interpretation.

Another problem is related to the qualitative change of the pattern type from SLS to structures with two L bands (LSL or SLSLS) with lower L-particle concentration γ at constant fill level ϕ. This is found at all fill levels where SLS have been identified. All mechanisms discussed above, however, are effective independent of the particle concentrations, since they consider only individual particle trajectories. The existence of the back sheet of S grains at low ϕ is confirmed experimentally for all concentrations γ. Thus, γ is not expected to affect the BS mechanism. The influence of γ on the flow profile and the SG mechanism has not been studied systematically yet, but definitely the shear gradient near the equatorial zone is always lower than in the lateral zones. In particular, even concentrations of less than $\gamma \approx 10\%$ of large beads can already trigger the transition from SLSLS to SLS at low-enough fill levels. For such low concentrations, the flow profile is almost identical to that of a granulate consisting of monodisperse S grains, and the SG mechanism drives large grains towards the poles. Thus, this mechanism cannot explain the observed transitions either.

In cylindrical mixers, it was suggested that the local composition of the mixture modifies the slope of the flowing layer (dynamic angle of repose) [28], and initial fluctuations of the dynamic angle of repose couple to a redistribution of grains. This mechanism can be responsible for band formation. In spherical mixers, this mechanism might add to the BS effect if the L grains form a compact surface coverage, thus stabilizing a central L stripe. We cannot verify this because with the present setup, variations in the dynamic angle of repose could not be determined.

The agglomeration of large grains in a central stripe could also be an indication of an attraction of large grains flowing in the top layer above a bed of small grains to regions covered predominantly with large grains. One can exclude direct particle-particle interactions since the material is definitely noncohesive. However, it was observed earlier that large particles embedded in a fine-grained material show a tendency to aggregate in a rotating tumbler [23]. A certain hint that regions covered preferentially by large grains attract neighboring trajectories of large grains in the flowing layer is found in Fig. 9. While the paths of individual L grains are redirected towards the equator when the grains are initially well mixed [Fig. 9(a)], the trajectories bend towards the lateral L stripes after the SLSLS bands have formed. In order to verify this idea, a systematic study of the trajectories of individual large grains in the spherical mixer will be necessary.

Recently, Zaman *et al.* [19] and D'Ortona *et al.* [20] described a secondary vortex flow of monodisperse grains in a spherical mixer, driving the particles towards the poles at the surface and towards the equator in the core of the granular bed. The same circulation may be present in the mixed systems, but it is not clear how it may influence the segregation process.

V. SUMMARY

We have shown that three types of segregation patterns form spontaneously in a spherical mixer filled with a bidisperse granular mixture of glass spheres. The container fill level and the composition of the granular mixture have equally strong influences on the segregation patterns observed in spherical mixers.

Some of the mechanisms proposed earlier for the selection of the segregation pattern type have been disproved or have been shown to be of minor importance. Instead, the main driving forces for the segregation patterns seem to be the SG and BS processes, a shear gradient induced drift of large particles out of the central band, and a counteracting motion of S particles towards the poles at low fill levels. A competition of these two processes may lead to the newly identified SLSLS bands. A full understanding of details of the pattern selection still lacks.

Due to the well-defined localization of the band patterns, this system deserves more than academic interest. It may also have some practical relevance for the separation of particles by size in a simple geometry. An advantage over long cylindrical mixers is that the bands form at well-defined positions for a given composition of the granular mixture.

ACKNOWLEDGMENTS

Sebastian Belau and Ines-Ute Grodrian are acknowledged for preparing samples and performing measurements. Kirsten Harth is cordially acknowledged for fruitful discussions and suggestions and for participation in some experiments. Financial support from the DAAD/MÖB researcher exchange program (Grant No. 64975) and the Hungarian Scientific Research Fund (Grant No. OTKA NN 107737) are acknowledged.

[1] Y. Oyama, Sci. Pap. Inst. Phys. Chem. Res. (Jpn.) **6**, 600 (1939); **37**, 17 (1940).
[2] E. Clément, J. Rajchenbach, and J. Duran, Europhys. Lett. **30**, 7 (1995).
[3] F. Cantelaube and D. Bideau, Europhys. Lett. **30**, 133 (1995).
[4] M. Nakagawa, S. A. Altobelli, C. Caprihan, and E. Fukushima, Chem. Eng. Sci. **52**, 4423 (1997).
[5] K. M. Hill, A. Caprihan, and J. Kakalios, Phys. Rev. Lett. **78**, 50 (1997).
[6] K. M. Hill, A. Caprihan, and J. Kakalios, Phys. Rev. E **56**, 4386 (1997).
[7] Z. Cui, Y. Zhao, Y. Chen, X. Liu, Z. Hua, C. Zhou, and J. Zheng, Particuology **13**, 128 (2014).
[8] M. Nakagawa, Chem. Eng. Sci. **49**, 2540 (1994).
[9] T. Finger, A. Voigt, J. Stadler, H. G. Niessen, L. Naji, and R. Stannarius, Phys. Rev. E **74**, 031312 (2006).
[10] S. J. Fiedor and J. M. Ottino, Phys. Rev. Lett. **91**, 244301 (2003).
[11] K. M. Hill and J. Kakalios, Phys. Rev. E **49**, R3610 (1994).
[12] N. A. Pohlman, J. M. Ottino, and R. M. Lueptow, Phys. Rev. E **74**, 031305 (2006).
[13] M. M. H. D. Arntz, W. K. den Otter, H. H. Beeftink, R. M. Boom, and W. J. Briels, Granular Matter **15**, 25 (2013).
[14] P. Chen, J. M. Ottino, and R. M. Lueptow, Phys. Rev. E **78**, 021303 (2008).
[15] P. Chen, J. M. Ottino, and R. M. Lueptow, New J. Phys. **13**, 055021 (2011).
[16] J. F. Gilchrist and J. M. Ottino, Phys. Rev. E **68**, 061303 (2003).
[17] L. Naji and R. Stannarius, Phys. Rev. E **79**, 031307 (2009).
[18] P. Chen, B. J. Lochman, J. M. Ottino, and R. M. Lueptow, Phys. Rev. Lett. **102**, 148001 (2009).
[19] Z. Zaman, U. DOrtona, P. B. Umbanhowar, J. M. Ottino, and R. M. Lueptow, Phys. Rev. E **88**, 012208 (2013).
[20] U. DOrtona, N. Thomas, Z. Zaman, and R. M. Lueptow, Phys. Rev. E **92**, 062202 (2015).
[21] N. A. Pohlman, S. W. Meyer, R. M. Lueptow, and J. M. Ottino, J. Fluid Mech. **560**, 355 (2006).
[22] G. Juarez, J. M. Ottino, and R. M. Lueptow, Phys. Rev. E **78**, 031306 (2008).
[23] I. Zuriguel, J. F. Boudet, Y. Amarouchene, and H. Kellay, Phys. Rev. Lett. **95**, 258002 (2005).
[24] T. Finger and R. Stannarius, Phys. Rev. E **75**, 031308 (2007).
[25] T. Arndt, T. Siegmann-Hegerfeld, S. J. Fiedor, J. M. Ottino, and R. M. Lueptow, Phys. Rev. E **71**, 011306 (2005).
[26] M. B. Donald and B. Roseman, British Chem. Eng. **7**, 749 (1962).
[27] S. Das Gupta, D. V. Khakhar, and S. K. Bhatia, Chem. Eng. Sci. **46**, 1513 (1991).
[28] O. Zik, D. Levine, S. G. Lipson, S. Shtrikman, and J. Stavans, Phys. Rev. Lett. **73**, 644 (1994).
[29] I. S. Aranson and L. S. Tsimring, Phys. Rev. Lett. **82**, 4643 (1999).
[30] I. S. Aranson, L. S. Tsimring, and V. M. Vinokur, Phys. Rev. E **60**, 1975 (1999).
[31] N. Taberlet and P. Richard, Phys. Rev. E **73**, 041301 (2006).
[32] S. Inagaki and K. Yoshikawa, Phys. Rev. Lett. **105**, 118001 (2010).
[33] Z. S. Khan, F. van Bussel, M. Schaber, R. Seemann, M. Scheel, and M. Di Michiel, New J. Phys. **13**, 105005 (2011).
[34] T. T. M. Nguyen, A. J. Sederman, M. D. Mantle, and L. F. Gladden, Phys. Rev. E **84**, 011304 (2011).
[35] C. P. Schlick, Y. Fan, P. B. Umbanhowar, J. M. Ottino, and R. M. Lueptow, J. Fluid Mech. **765**, 632 (2015).
[36] T. Finger, M. Schröter, and R. Stannarius, New J. Phys. **17**, 093023 (2015).
[37] Z. S. Khan, W. A. Tokaruk, and S. W. Morris, Europhys. Lett. **66**, 212 (2004).
[38] P. Chen, J. M. Ottino, and R. M. Lueptow, Phys. Rev. Lett. **104**, 188002 (2010).
[39] N. Taberlet, W. Losert, and P. Richard, Europhys. Lett. **68**, 522 (2004).
[40] D. Fischer, T. Finger, F. Angenstein, and R. Stannarius, Phys. Rev. E **80**, 061302 (2009).
[41] H. P. Kuo, Y. C. Hsiao, and P. Y. Shih, Powder Technol. **166**, 161 (2006).
[42] N. A. Pohlman, B. L. Severson, J. M. Ottino, and R. M. Lueptow, Phys. Rev. E **73**, 031304 (2006).
[43] D. C. Rapaport, Phys. Rev. E **65**, 061306 (2002).
[44] D. C. Rapaport, Phys. Rev. E **75**, 031301 (2007).
[45] V. Frette and J. Stavans, Phys. Rev. E **56**, 6981 (1997).
[46] M. Nakagawa, S. A. Altobelli, C. Caprihan, E. Fukushima, and E.-K. Jeong, Exp. Fluids **16**, 54 (1993).
[47] K. M. Hill and J. Kakalios, Phys. Rev. E **52**, 4393 (1995).
[48] K. M. Hill, D. V. Khakhar, J. F. Gilchrist, J. J. McCarthy, and J. M. Ottino, Proc. Natl. Acad. Sci. USA **96**, 11701 (1999).
[49] K. M. Hill, N. Jain, and J. M. Ottino, Phys. Rev. E **64**, 011302 (2001).
[50] K. Choo, T. C. A. Molteno, and S. W. Morris, Phys. Rev. Lett. **79**, 2975 (1997).
[51] K. Choo, M. W. Baker, T. C. A. Molteno, and S. W. Morris, Phys. Rev. E **58**, 6115 (1998).
[52] N. Jain, D. V. Khakhar, R. M. Lueptow, and J. M. Ottino, Phys. Rev. Lett. **86**, 3771 (2001).
[53] A. Alexander, F. J. Muzzio, and T. Shinbrot, Granul. Matter **5**, 171 (2004).
[54] Z. S. Khan and S. W. Morris, Phys. Rev. Lett. **94**, 048002 (2005).
[55] L. Prigozhin and H. Kalman, Phys. Rev. E **57**, 2073 (1998).
[56] S. J. Fiedor, P. Umbanhowar, and J. M. Ottino, Phys. Rev. E **73**, 041303 (2006).
[57] S. W. Meier, R. M. Lueptow, and J. M. Ottino, Adv. Phys. **56**, 757 (2007).
[58] S. Massol-Chaudeur, H. Berthiaux, and J. A. Dodds, Chem. Eng. Sci. **57**, 4053 (2002).
[59] Yi Fan and K. M. Hill, New J. Phys. **13**, 095009 (2011).
[60] Yi Fan and K. M. Hill, Phys. Rev. Lett. **106**, 218301 (2011).